Atmos. Chem. Phys. Discuss., doi:10.5194/acp-2016-820, 2016
Manuscript under review for journal Atmos. Chem. Phys.
Published: 19 September 2016

Atmospheric Chemistry and Physics Discussions

Constraining uncertainties in particle wall-deposition correction during SOA formation in chamber experiments

T. Nah,[1] R. C. McVay,[2] J.R. Pierce,[3] J. H. Seinfeld[2,4] and N. L. Ng[1,5*]

[1]*School of Chemical and Biomolecular Engineering, Georgia Institute of Technology, Atlanta, GA, USA*
[2]*Division of Chemistry and Chemical Engineering, California Institute of Technology, Pasadena, CA, USA*
[3]*Depratment of Atmospheric Science, Colorado State University, Fort Collins, CO, USA*
[4]*Division of Engineering and Applied Science, California Institute of Technology, Pasadena, CA, USA*
[5]*School of Earth and Atmospheric Sciences, Georgia Institute of Technology, Atlanta, GA, USA*

** To whom correspondence should be addressed: ng@chbe.gatech.edu*

Abstract

The effect of vapor wall-deposition on secondary organic aerosol (SOA) formation has gained significant attention; however, uncertainties in experimentally derived SOA mass yields due to uncertainties in particle wall-deposition remain. Different approaches have been used to correct for particle wall-deposition in SOA-formation studies, each having its own set of assumptions in determining the particle wall-loss rate. In volatile and intermediate-volatility organic compound systems in which SOA formation is governed by kinetically limited growth, the effect of vapor wall-deposition on SOA mass yields can be constrained by using high surface area concentrations of seed aerosol to promote the condensation of SOA-forming vapors onto seed aerosol instead of the chamber walls. However, under such high seed aerosol levels, the presence of significant coagulation may complicate the particle wall-deposition correction. Here, we present a model framework that accounts for coagulation in chamber studies in which high seed aerosol surface area concentrations are used. For the α-pinene ozonolysis system, we find that, after accounting for coagulation, SOA mass yields remain approximately constant when large seed aerosol surface area concentrations ($\geq$ 8000 μm^2 cm^{-3}) are used, consistent with our prior study (Nah et al., 2016) that α-pinene ozonolysis SOA formation is governed by quasi-equilibrium growth. In addition, we systematically assess the uncertainties in the calculated SOA mass concentrations and yields between four different particle wall-loss correction methods over the series of α-pinene ozonolysis experiments. At low seed aerosol surface area concentrations ($<$ 3000 μm^2 cm^{-3}), the SOA mass yields at peak SOA growth obtained from the particle wall-loss correction

Atmos. Chem. Phys. Discuss., doi:10.5194/acp-2016-820, 2016
Manuscript under review for journal Atmos. Chem. Phys.
Published: 19 September 2016

Atmospheric Chemistry and Physics Discussions

methods agree within 14 %. However, at high seed aerosol surface area concentrations (≥ 8000 μm^2 cm^{-3}), the SOA mass yields at peak SOA growth obtained from different particle wall-loss correction methods can differ by as much as 58 %. These differences arise from assumptions made in the particle wall-loss correction regarding the first-order particle wall-loss rate. This study highlights the importance of accounting for particle wall-deposition accurately during SOA-formation chamber experiments and assessing the uncertainties associated with the application of the particle wall-deposition correction method when comparing and using SOA mass yields measured in different studies.

1. Introduction

Secondary organic aerosol (SOA), which constitutes a large mass fraction of fine atmospheric particulate matter, is formed from the oxidation of volatile and intermediate-volatility organic compounds (VOCs and IVOCs) followed by gas-particle partitioning (Kanakidou et al., 2005; Kroll and Seinfeld, 2008; Hallquist et al., 2009; Tsigaridis et al., 2014). Laboratory chambers are typically used to study SOA formation from VOC and IVOC oxidation in a controlled environment. SOA mass yields (Y), defined as the ratio of mass concentration of SOA formed (ΔM_o) to the mass concentration of reacted hydrocarbon (ΔHC) ($Y = \Delta M_o/\Delta HC$), are measured in these chamber experiments (Odum et al., 1996; Odum et al., 1997a; Odum et al., 1997b). Interpretation of data derived from such experiments is complicated by the fact that particles and SOA-forming vapors deposit on the chamber walls throughout an experiment (Crump and Seinfeld, 1981; McMurry and Grosjean, 1985; McMurry and Rader, 1985; Cocker et al., 2001; Weitkamp et al., 2007; Pierce et al., 2008; Hildebrandt et al., 2009; Loza et al., 2010; Matsunaga and Ziemann, 2010; Loza et al., 2012; Kokkola et al., 2014; McVay et al., 2014; Yeh and Ziemann, 2014; Zhang et al., 2014; Yeh and Ziemann, 2015; Zhang et al., 2015; Krechmer et al., 2016; La et al., 2016; McVay et al., 2016; Ye et al., 2016; Nah et al., 2016). Failure to account for particle and vapor wall-losses accurately will result in incorrect SOA mass yields, which will lead to flawed predictions of ambient SOA mass concentrations (Cappa et al., 2016).

Particles deposit on the chamber walls via diffusion, gravitational settling and electrostatic forces (Crump and Seinfeld, 1981; McMurry and Grosjean, 1985; McMurry

Atmos. Chem. Phys. Discuss., doi:10.5194/acp-2016-820, 2016
Manuscript under review for journal Atmos. Chem. Phys.
Published: 19 September 2016

Atmospheric Chemistry and Physics Discussions

and Rader, 1985; Pierce et al., 2008). The rate at which particles deposit on chamber walls depends on particle size. The particle wall-loss mechanism for uncharged particles in an uncharged chamber is similar to that of the dry deposition of particles (Pierce et al., 2008; Seinfeld and Pandis, 2016). Small particles are transported by Brownian diffusion through the boundary layer adjacent to the chamber walls, while the loss of large particles is governed by gravitational settling. Particle wall-loss rates are enhanced if the particles and/or chamber walls are charged (McMurry and Grosjean, 1985; McMurry and Rader, 1985; Pierce et al., 2008). Smaller charged particles deposit more efficiently than larger charged particles due to their larger Brownian diffusion rates and charge-to-mass ratios.

Several methods have been used to account for particle wall-deposition in SOA-formation studies. In one particle wall-loss correction method, the rate of decay of polydisperse inert seed aerosol (e.g., ammonium sulfate particles) is measured in periodic seed-only experiments (Keywood et al., 2004; Pierce et al., 2008). Size-dependent particle wall-deposition coefficients are then obtained by fitting a first-order exponential decay to the measured particle number concentration decay in each size bin. The total aerosol number concentration usually needs to be sufficiently low in these seed-only experiments such that the effect of coagulation is negligible. In cases in which high seed aerosol number concentrations are used, an aerosol dynamics model can be applied to correct the particle wall-deposition coefficients for coagulation. Particle wall-loss in a SOA formation experiment is then accounted for using these size-dependent particle wall-deposition coefficients to obtain the total SOA mass concentration. A key assumption of this approach is that the size-dependent particle wall-deposition coefficients do not change between these seed-only and SOA-formation experiments. Other previously reported particle wall-loss correction methods do not require the use of separate seed-only experiments to characterize particle wall-loss rates. Instead, the average loss rate of the total aerosol mass or number concentration is measured directly during the SOA formation experiment (Carter et al., 2005; Pathak et al., 2007; Pierce et al., 2008; Hildebrandt et al., 2009). The measured average particle loss rate is then applied to the entire experiment to correct for particle wall-deposition. A key assumption of this approach is that the particle wall-loss rate is not strongly dependent on particle size, thus allowing for the overall particle wall-loss to be characterized by a single decay

Atmos. Chem. Phys. Discuss., doi:10.5194/acp-2016-820, 2016
Manuscript under review for journal Atmos. Chem. Phys.
Published: 19 September 2016

Atmospheric Chemistry and Physics Discussions

rate coefficient. The extent to which these methods account for particle wall-deposition in SOA-formation studies performed in a chamber, in which particle wall-loss rates are known to strongly depend on particle size, is unclear. Therefore, SOA mass yield uncertainties associated with the application of different particle wall-loss correction methods need to be evaluated when comparing and using SOA mass yields measured in different studies. This is the subject of the present work.

Previous studies have shown that SOA mass yields can be substantially underestimated if the loss of SOA-forming vapors to chamber walls is not accounted for (Matsunaga and Ziemann, 2010; McVay et al., 2014; Yeh and Ziemann, 2014; Zhang et al., 2014; Yeh and Ziemann, 2015; Zhang et al., 2015; Krechmer et al., 2016; La et al., 2016; McVay et al., 2016; Ye et al., 2016; Nah et al., 2016). Unlike particle wall-loss, experimental methods for estimating vapor wall-loss rates in chambers are not yet well established. However, the extent to which vapor wall-loss impacts SOA mass yields can be characterized and quantified using time-dependent, parameterizable models that use the measured SOA mass concentrations as model inputs (Zhang et al., 2014). Recent studies have shown that the addition of large concentrations of seed aerosol can promote gas-particle partitioning, and consequently increase SOA mass yields in VOC systems where the condensation of SOA-forming vapors onto seed aerosol is kinetically limited (i.e., the timescale for gas-particle equilibrium is competitive with or greater than those for reaction and vapor wall-loss) (Riipinen et al., 2011; Zhang et al., 2012; McVay et al., 2014; Zhang et al., 2014). In contrast, SOA growth is independent of seed aerosol surface area in VOC systems in which the condensation of SOA-forming vapors onto seed aerosol is governed by quasi-equilibrium growth (i.e., the timescale for gas-particle equilibrium is less than those for reaction and vapor wall-loss) (Riipinen et al., 2011; Zhang et al., 2012; McVay et al., 2014; McVay et al., 2016; Nah et al., 2016). Together, these studies show that the role of gas-particle partitioning (i.e., kinetically limited vs. quasi-equilibrium SOA growth) in influencing vapor wall-deposition can be inferred from the relationship between SOA mass yields and seed aerosol surface area. However, the use of high seed aerosol surface area concentrations in chamber studies may complicate the particle wall-loss correction since (depending on the particle wall-loss correction method used) the role of coagulation may need to be accounted for. It also

Atmos. Chem. Phys. Discuss., doi:10.5194/acp-2016-820, 2016
Manuscript under review for journal Atmos. Chem. Phys.
Published: 19 September 2016

128 needs to be established how particle wall-deposition rates may change when different
129 seed aerosol concentrations (i.e., number, surface area and volume concentrations) and
130 size distributions are used. These uncertainties underscore the need to better constrain the
131 uncertainties associated with particle wall-loss correction since this correction will affect
132 the evaluation of the magnitude by which vapor wall-loss impacts chamber-derived SOA
133 mass yields.

134 In this work, we present results from targeted chamber experiments demonstrating
135 the change of size-dependent particle wall-deposition rates with different seed aerosol
136 concentrations (i.e., number, surface area and volume concentrations) and size
137 distributions. We also demonstrate how coagulation can be (and needs to be) accounted
138 for in experiments in which high seed aerosol surface area concentrations are used to
139 promote the condensation of SOA-forming vapors onto seed aerosol. Finally, we
140 compare SOA mass concentrations and yields in the canonical α-pinene ozonolysis
141 system obtained using four different particle wall-deposition correction methods, and
142 examine the uncertainties associated with each method.

143 **2. Experimental**

144 Experiments were carried out in the Georgia Tech Environmental Chamber
145 (GTEC) facility (Boyd et al., 2015). A single FEP Teflon chamber (volume 13 m^3) was
146 used for the entire study. Prior to each experiment, the chamber was flushed with dried,
147 purified air for > 24 h until the aerosol number concentration was < 30 cm^{-3}. Experiments
148 were performed at < 5 % RH and 25 °C. NO_x mixing ratios in these experiments were < 1
149 ppb.

150 The dark α-pinene ozonolysis experimental procedure used in this study was
151 similar to that used in Nah et al. (2016). First, 22 ppm of cyclohexane (Sigma Aldrich, ≥
152 99.9 %), which served as an OH scavenger (~440 times the initial α-pinene
153 concentration), was injected into the chamber. Based on the cyclohexane and α-pinene
154 concentrations in the chamber, the reaction rate of OH with cyclohexane is ~60 times
155 greater than that with α-pinene. Ammonium sulfate (AS) seed aerosol was next
156 introduced into the chamber via atomization of an aqueous AS solution. A known

Atmos. Chem. Phys. Discuss., doi:10.5194/acp-2016-820, 2016
Manuscript under review for journal Atmos. Chem. Phys.
Published: 19 September 2016

Atmospheric Chemistry and Physics Discussions

concentration of α-pinene (Sigma Aldrich, > 99 %) (~50 ppb in all experiments) was then injected into the chamber. Finally, 500 ppb of ozone (O_3), which was generated by passing purified air into a photochemical cell (Jelight 610), was introduced into the chamber for 54.25 min after the seed aerosol and α-pinene concentrations in the chamber had stabilized. The beginning of O_3 injection into the chamber marked the start of the reaction (i.e., reaction time = 0 min). The O_3 mixing timescale was ~12 min for all experiments. The O_3 injection time and mixing timescale were determined from separate O_3-only experiments (Nah et al., 2016). In seed-only experiments performed to measure size-dependent particle wall-deposition coefficients, only AS seed aerosol was introduced into the chamber. A gas chromatograph-flame ionization detector (GC-FID, Agilent 7890A) and O_3 monitor (Teledyne T400) measured the α-pinene and O_3 concentrations, respectively. GC-FID measurements were taken 15 min apart. A high-resolution time-of-flight aerosol mass spectrometer (HR-ToF-AMS, Aerodyne Research Inc.) measured the aerosol elemental composition (DeCarlo et al., 2006; Canagaratna et al., 2015). A scanning mobility particle sizer (SMPS, TSI), which consists of a differential mobility analyzer (DMA, TSI 3081) and a condensation particle counter (CPC, TSI 3775), measured the aerosol size distributions, number and volume concentrations.

The initial total AS seed aerosol surface area concentrations used in this study were ~1000 and ≥ 8000 $\mu m^2\ cm^{-3}$ (referred to as "low-SA" and "high-SA" experiments, respectively). To investigate how the seed aerosol size distribution may affect SOA mass concentrations and yields, two different concentrations of AS solutions were used to generate AS seed aerosol for both the seed-only and α-pinene ozonolysis experiments: 0.015 M or 0.05 M. In some experiments, both the 0.015 and 0.05 M AS solutions were atomized into the chamber to achieve the desired total AS seed aerosol surface area concentration. In these experiments, the 0.015 M AS solution was first atomized into the chamber to achieve about half of the desired total AS seed aerosol surface area concentration, followed by atomization of the 0.05 M AS solution. A summary of the experimental conditions is shown in Table 1.

3. Aerosol dynamics model

Atmos. Chem. Phys. Discuss., doi:10.5194/acp-2016-820, 2016
Manuscript under review for journal Atmos. Chem. Phys.
Published: 19 September 2016

Atmospheric Chemistry and Physics Discussions

An aerosol dynamics model is used to determine particle wall-deposition coefficients that have been corrected for coagulation. This model was first described in Pierce et al. (2008). In our work, we do not use the full Aerosol Parameter Estimation (APE) model described in Pierce et al. (2008), but rather we use the model used to create the "No condensation" curve in Fig. 5 of the paper. This model includes only coagulation and particle wall-loss, and it assumes that no condensation or evaporation occurs during seed-only experiments, which are especially designed to measure particle wall-deposition rates (experiments 1 through 6 in Table 1). Coagulation coefficients are calculated from Table 13.1 in Seinfeld and Pandis (2016). The inputs to the model are the raw time-dependent number distribution data measured by the SMPS during a particular seed-only experiment. For each time step of the SMPS measurements, the model calculates the decrease in the number concentration in each particle size bin due solely to coagulation. The difference between this calculated decrease and the observed decrease in the number concentration is attributed to particle wall-deposition, thus allowing size-dependent particle wall-deposition coefficients to be determined. The model then re-calculates the decrease in the number concentration for each particle size bin for that time step due to both coagulation and particle wall-deposition using the deposition coefficients just determined. The calculated decrease in the number concentration is again compared to the measured values. This process of finding the size-dependent particle wall-deposition rates is iterated using Newton's method in order to converge upon particle wall-deposition coefficients that fit the calculated number concentration decay to the observed decay. The process is repeated for each SMPS measurement time step, yielding size- and time-dependent particle wall-deposition coefficients. This process of finding the size-dependent particle wall-deposition rates is carried out only when the number concentration in the particle size bin of interest is > 20 particles cm^{-3}. For bins with ≤ 20 particles cm^{-3}, the deposition coefficient is not calculated during these time steps due to uncertainties in the number counts in these bins leading to low confidence in the determined particle wall-deposition rates. The deposition coefficients are averaged over the entire experiment to yield coagulation-corrected size-dependent particle wall-deposition coefficients.

4. Results and discussion

Atmos. Chem. Phys. Discuss., doi:10.5194/acp-2016-820, 2016
Manuscript under review for journal Atmos. Chem. Phys.
Published: 19 September 2016

4.1. Role of coagulation in particle wall-deposition corrections

We performed a set of seed-only experiments using 0.015 M AS and/or 0.05 M AS solutions to determine the extent to which size-dependent particle wall-loss rates change with different seed aerosol concentrations and size distributions (experiments 1 through 6 in Table 1). The initial total AS seed aerosol surface area concentrations in the low-SA-seed-only and high-SA-seed-only experiments are similar to those used in the α-pinene ozonolysis experiments (i.e., ~1000 and ≥ 8000 $\mu m^2\ cm^{-3}$, respectively). Figure S1 shows the initial and final (420 min) number and volume size distributions for the seed-only experiments. The initial number and volume size distributions in the low-SA-seed-only experiments are smaller than those in the high-SA-seed-only experiments, regardless of the concentration of the AS solution used to generate seed aerosol. As expected, all of the size distributions shift to larger particle diameters as the experiment progresses due to more efficient loss of smaller particles to the chamber walls and via coagulation as compared to larger particles.

Figure 1 shows the size-dependent particle wall-deposition coefficients measured directly in the low-SA-seed-only and high-SA-seed-only experiments (dashed lines). We will refer to them as the *uncorrected* size-dependent particle wall-deposition coefficients for the remainder of the discussion in this work since the effect of coagulation is assumed to be negligible, and thus coagulation is not corrected for in these coefficients. The uncorrected size-dependent particle wall-deposition coefficients are obtained directly from SMPS measurements by fitting a first-order exponential decay to the measured particle number concentration decay in each size bin. The uncorrected particle wall-deposition coefficients are compared to those corrected for coagulation (shown as solid lines in Fig. 1), which are obtained from the application of the aerosol dynamics model (described in section 3) to the number distribution data measured by the SMPS. As anticipated, a comparison of the uncorrected and coagulation-corrected size-dependent particle wall-deposition coefficients indicates that coagulation has a smaller effect on the deposition coefficients from the low-SA-seed-only experiments (experiments 1 through 4) compared to the high-SA-seed-only experiments (experiments 5 and 6). For example, for particle diameters > 400 nm, the coagulation-corrected deposition coefficients for the

Atmos. Chem. Phys. Discuss., doi:10.5194/acp-2016-820, 2016
Manuscript under review for journal Atmos. Chem. Phys.
Published: 19 September 2016

high-SA-seed-only experiments are up to an order of magnitude faster than the uncorrected deposition coefficients. The smaller uncorrected deposition coefficients can be attributed to particle formation (via coagulation) occurring simultaneously with particle wall-deposition at these larger particle diameters in the high-SA-seed-only experiments. A comparison of the change in total particle number concentration due to coagulation alone (Fig. S2) shows that the low-SA-seed-only experiments (experiments 1 through 4) have smaller coagulation rates than the high-SA-seed-only experiments (experiments 5 and 6). The observation that coagulation has a smaller effect on the inferred deposition coefficients in the low-SA-seed-only experiments is expected since these experiments involve significantly smaller particle number concentrations as compared to the high-SA-seed-only experiments (2.5 to 4 x 10^4 particles cm^{-3} vs. 1 to 1.3 x 10^5 particles cm^{-3}).

The coagulation-corrected size-dependent particle wall-deposition coefficients obtained from the low-SA-seed-only experiments are generally in agreement. This is also the case for the coagulation-corrected particle wall-deposition coefficients obtained from the high-SA-seed-only experiments. Similar trends are observed for the uncorrected size-dependent particle wall-deposition coefficients. Therefore, the concentration of the AS solution(s) (i.e., 0.015 M and/or 0.05 M) used to generate the seed aerosol in seed-only experiments does not influence the size-dependent particle wall-deposition coefficients. The coagulation-corrected size-dependent particle wall-deposition coefficients obtained from the low-SA-seed-only experiments are different from those obtained from the high-SA-seed-only experiments. In addition, the minimum coagulation-corrected particle wall-deposition coefficient for the low-SA-seed-only experiment (minimum particle diameter ~300 nm) is lower than that of the high-SA-seed-only experiments (minimum particle diameter ~530 nm). This result is surprising since the particle wall-deposition coefficients are expected to depend solely on particle size once coagulation is accounted for.

We identify two possible explanations for the differences in the coagulation-corrected particle wall-deposition coefficients. The first possibility is that there is a difference in particle charging of the seed aerosol in the low-SA-seed-only and high-SA-seed-only experiments. Particle wall-deposition is enhanced when charges are present on

Atmos. Chem. Phys. Discuss., doi:10.5194/acp-2016-820, 2016
Manuscript under review for journal Atmos. Chem. Phys.
Published: 19 September 2016

Atmospheric Chemistry and Physics Discussions

277 particles (McMurry and Grosjean, 1985; McMurry and Rader, 1985; Pierce et al., 2008).
278 In all our experiments, a Boltzmann charge distribution was applied to the AS seed
279 aerosol by passing the particles through a Po-210 neutralizer prior to injection into the
280 chamber. However, it is possible that the particles are not fully neutralized before
281 entering the chamber, resulting in a difference in the true particle wall-deposition
282 coefficients due to the differences in particle charging between the experiments.

283 The second possible explanation for the differences in the coagulation-corrected
284 particle wall-deposition coefficients is that the Brownian coagulation kernel that we used
285 for our coagulation correction may not account for all of the coagulation in the chamber.
286 Coulombic and/or van der Walls forces may enhance the coagulation rates. We
287 performed a series of simple sensitivity tests to determine how the coagulation-corrected
288 size-dependent particle wall-deposition coefficients change as a function of coagulation
289 coefficients. In these tests, we scale our Brownian coagulation kernel by 1.1 and 1.5
290 uniformly across all particle sizes (as Coulombic and van der Waals enhancements to
291 coagulation have size dependence, these simple sensitivity tests do not fully capture the
292 changes due to either of these forces). Figure S3 shows results from sensitivity tests
293 performed on the seed-only experiments. These sensitivity tests show that the
294 coagulation-corrected particle wall-deposition coefficients in the low-SA-seed-only and
295 high-SA-seed-only experiments converge towards each other with increasing scale
296 factors on coagulation. However, with increasing coagulation scale factors, our derived
297 wall-deposition coefficients become negative at some particle sizes, which implies that
298 the size-independent coagulation scale factors are unrealistic. Future work should include
299 a more detailed investigation of the size-dependent coagulation enhancements provided
300 by Coulombic and van der Waals forces (which in turn requires knowledge about the
301 charge distribution and van der Waals forces), and it should include an investigation of
302 the change-enhanced particle wall-losses (again requiring a knowledge of the charge
303 distribution). For the remainder of this work, we will use coagulation-corrected particle
304 wall-deposition coefficients with no enhancement to the coagulation rates (solid lines in
305 Figs. 1 and S3a).

Atmos. Chem. Phys. Discuss., doi:10.5194/acp-2016-820, 2016
Manuscript under review for journal Atmos. Chem. Phys.
Published: 19 September 2016

306 We evaluated the effectiveness of the coagulation-corrected particle wall-
307 deposition coefficients (with no scaling of Brownian coagulation) in correcting for
308 particle wall-loss and coagulation by applying these coefficients to the SMPS data from
309 the seed-only experiments. The corrected volume concentration should level off at a
310 constant value (at the initial particle volume concentration) when particle wall-deposition
311 and coagulation are properly accounted for, since no condensation or evaporation occurs
312 during these experiments (due to the use of low-volatility AS seed aerosol and the
313 absence of condensable gases) and the wall-deposited particle volume concentration is
314 added back to the suspended particle volume concentration during particle wall-loss
315 correction. Figure S4 shows the raw and particle wall-deposition-corrected volume
316 concentrations. Coagulation-corrected size-dependent particle wall-deposition
317 coefficients are used for the particle wall-deposition correction shown in Fig. S4. Over all
318 experiments, the particle wall-deposition-corrected final volume concentration (i.e., at the
319 end of the experiment) is within 1 to 5 % of the initial volume concentration (Table S1).

320 **4.2. α-pinene ozonolysis**

321 We use the "size-dependent" method described in Loza et al. (2012) and Nah et
322 al. (2016) to correct for particle wall-deposition in the α-pinene ozonolysis experiments.
323 Briefly, size-dependent particle wall-deposition coefficients determined in separate seed-
324 only experiments (either through direct measurements or using an aerosol dynamics
325 model) are used to correct for particle wall-deposition in SOA-formation experiments.
326 Here we assume that particles cease to uptake SOA-forming vapors once they have
327 deposited, and hence the SOA mass present on deposited particles does not increase after
328 deposition. A key assumption of the "size-dependent" method is that the size-dependent
329 particle wall-deposition coefficients do not change significantly between experiments.
330 Seed-only experiments are performed regularly in the GTEC chamber. As shown in Fig.
331 1 (and Fig. 1 of Nah et al. (2016)), the uncorrected and coagulation-corrected size-
332 dependent particle wall-deposition coefficients are generally in line with each other at a
333 given seed aerosol surface area concentration. Since the seed-only and α-pinene
334 ozonolysis experiments were performed under similar experimental conditions (i.e., dark
335 conditions at < 5 % RH and 25 °C), the size-dependent particle wall-deposition

Atmos. Chem. Phys. Discuss., doi:10.5194/acp-2016-820, 2016
Manuscript under review for journal Atmos. Chem. Phys.
Published: 19 September 2016

coefficients are not expected to change significantly with reaction conditions for the experiments presented in this study.

Since the focus of this work is the influence of coagulation and particle wall-deposition on SOA mass yields, more high-SA α-pinene ozonolysis experiments (experiments 9 through 12) were performed than low-SA experiments (experiments 7 and 8). To investigate the influence of coagulation on the SOA mass yields, both the uncorrected and coagulation-corrected size-dependent particle wall-deposition coefficients are used to correct for particle wall-deposition in the α-pinene ozonolysis experiments. All the low-SA α-pinene ozonolysis data are particle wall-deposition-corrected using uncorrected and coagulation-corrected size-dependent particle wall-deposition coefficients from the low-SA-seed-only experiments, and all the high-SA α-pinene ozonolysis data are corrected using uncorrected and coagulation-corrected particle wall-deposition coefficients from the high-SA-seed-only experiments. Additional details regarding the size-dependent particle wall-deposition coefficients used to correct for particle wall-deposition in the different α-pinene ozonolysis experiments are provided in Table 1. Figure S5 shows the raw and particle wall-deposition-corrected aerosol volume concentrations for all the α-pinene ozonolysis experiments. In all the α-pinene ozonolysis experiments, the volume concentrations that have been particle wall-deposition-corrected using coagulation-corrected size-dependent particle wall-deposition coefficients (black) reach peak values at reaction time ~100 min. In contrast, volume concentrations that have been particle wall-deposition-corrected using uncorrected size-dependent particle wall-deposition coefficients (blue) increase monotonically in the high-SA experiments (experiments 9 through 12).

The SOA mass concentration is calculated from the product of the SOA density with the difference of the particle wall-deposition-corrected volume concentration and the initial seed aerosol volume concentration. We use an SOA density of 1.37 g cm^{-3}, which was previously measured by Nah et al. (2016). Figure 2 shows the reaction profiles of the low-SA α-pinene ozonolysis experiments. The SOA mass concentrations obtained using the coagulation-corrected (Figs. 2a and 2b) and uncorrected (Figs. 2c and 2d) size-dependent particle wall-deposition coefficients are sufficiently similar, which suggests

Atmos. Chem. Phys. Discuss., doi:10.5194/acp-2016-820, 2016
Manuscript under review for journal Atmos. Chem. Phys.
Published: 19 September 2016

that coagulation plays a minor role in the low-SA experiments. As reported in Nah et al. (2016), SOA growth typically occurs within 10 to 20 min of the start of the reaction. The molar ratio of O_3 reacted to α-pinene reacted is approximately 1:1 (i.e., 50 ppb α-pinene reacted with 50 ppb O_3), which indicates that O_3 reacts with α-pinene and not its oxidation products. All the α-pinene reacts within 90 to 100 min of the start of reaction in the 500 ppb O_3 experiments, and peak SOA levels occur at reaction time ~100 min. SOA growth basically ceases once all the α-pinene has reacted, indicating that the first step of α-pinene ozonolysis is rate-limiting and the first-generation products are condensable (Ng et al., 2006; Chan et al., 2007). This result is expected since α-pinene has a single double bond. The slight decrease in the SOA mass concentrations after peak SOA growth may be due to imperfections in the particle wall-deposition correction and/or vapor wall-deposition.

Figure 3 shows the reaction profiles of the high-SA α-pinene ozonolysis experiments. In cases where the coagulation-corrected size-dependent particle wall-deposition coefficients are used to correct for particle wall-deposition (Figs. 3a-d), the SOA growth profile is similar to that of the low-SA experiments; SOA growth essentially stops once all the α-pinene has reacted. In contrast, when the uncorrected size-dependent particle wall-deposition coefficients are used to correct for particle wall-deposition (Figs. 3e-h), the SOA mass concentration continues to increase even after all the α-pinene has reacted. This indicates that for the "size-dependent" method, SOA mass concentrations, and consequently SOA mass yields, can be substantially overestimated when coagulation is not accounted for during particle wall-deposition correction in high-SA experiments. This underscores the importance of accounting for coagulation and particle wall-deposition appropriately in chamber studies that employ high seed aerosol concentrations. We will use SOA mass concentrations corrected using coagulation-corrected size-dependent particle wall-deposition coefficients (solid lines in Fig. 1) for the remainder of the discussion in this work.

Figure 4 shows the time-dependent SOA mass yields as a function of initial seed aerosol surface area concentration for the α-pinene ozonolysis experiments. Also included in Fig. 4 are results from Nah et al. (2016); SOA mass concentrations obtained

Atmos. Chem. Phys. Discuss., doi:10.5194/acp-2016-820, 2016
Manuscript under review for journal Atmos. Chem. Phys.
Published: 19 September 2016

using coagulation-corrected size-dependent particle wall-deposition coefficients determined in their study (Fig. S7 of Nah et al. (2016)). The SOA mass yield at peak SOA growth remains approximately constant even at seed aerosol surface area concentrations ≥ 8000 μm^2 cm^{-3}. This confirms conclusions from our previous study that the seed aerosol surface area concentration does not influence the partitioning of gas-phase products to the particle phase in the α-pinene ozonolysis system (Nah et al., 2016). As discussed in Nah et al. (2016), this behavior arises because SOA formation in the α-pinene ozonolysis system is dominated by quasi-equilibrium growth (Saleh et al., 2013), which occurs when the production rate of SOA-forming vapors is significantly slower than that required to establish gas-particle equilibrium (Riipinen et al., 2011; Shiraiwa and Seinfeld, 2012; Zhang et al., 2012). Gas-particle equilibrium is governed by the amount of organic material in the system when the vapor and particle phases maintain equilibrium. Thus, the seed aerosol surface area does not control the condensation rate of SOA-forming vapors (McVay et al., 2014).

It is important to note that when the uncorrected size-dependent particle wall-deposition coefficients (dashed lines in Fig. 1) are used for the particle wall-deposition correction, the SOA mass yield at peak SOA growth increases with seed aerosol surface area (Fig. S6). This trend would lead to the incorrect conclusion that SOA formation in the α-pinene ozonolysis system is governed by kinetically limited growth. Therefore, this result further highlights the importance of accounting for coagulation and particle wall-deposition properly in chamber studies (especially when high number concentrations of seed aerosol are used) to avoid erroneous conclusions regarding the role of gas-particle partitioning (quasi-equilibrium vs. kinetically limited SOA growth) in affecting vapor wall-deposition and SOA mass yields in VOC systems.

4.3. Uncertainties in SOA mass concentrations due to particle wall-loss corrections

In the previous section, we showed that ignoring the role of coagulation in the "size-dependent" particle wall-deposition correction method can contribute significant errors to the calculated SOA mass concentrations and yields. These uncertainties could lead to erroneous conclusions regarding the role of gas-particle partitioning in influencing vapor wall-loss in the VOC system. Here, we investigate the uncertainties in the SOA

Atmos. Chem. Phys. Discuss., doi:10.5194/acp-2016-820, 2016
Manuscript under review for journal Atmos. Chem. Phys.
Published: 19 September 2016

mass concentrations and yields as a result of the use of different particle wall-deposition correction methods. We analyzed data from the α-pinene ozonolysis experiments using four different particle wall-deposition correction methods. SOA mass concentrations and yields obtained using the "size-dependent" particle wall-deposition correction method (discussed in section 4.2) are compared to those obtained using the "number averaged", "volume averaged" and "inert tracer" methods, which are described previously by Carter et al. (2005), Pathak et al. (2008) and Hildebrandt et al. (2009), respectively. For the "size-dependent" method, only SOA mass concentrations and yields corrected using coagulation-corrected size-dependent particle wall-deposition coefficients (Fig. 4) will be used in the discussion presented here.

The "number averaged" and "volume averaged" methods use SMPS measurements taken during SOA-formation studies. The "number averaged" method involves measuring the average loss rate of the total aerosol number concentration after peak SOA growth and then applying this first-order particle wall-deposition rate to the entire experiment to correct for particle wall-loss (Carter et al., 2005). Since the average loss rate of the total aerosol volume concentration is assumed to be the same as that of the total aerosol number concentration, this first-order particle wall-deposition rate is also applied to the total aerosol volume concentration data to determine the SOA mass concentration. The "volume averaged" method involves measuring the average loss rate of the total aerosol volume or mass concentration after peak SOA growth, and then applying this first-order particle wall-deposition rate to the entire experiment to correct for particle wall-loss (Pathak et al., 2007). Since the particle wall-deposition rate is directly measured during SOA-formation experiments in the "number averaged" and "volume averaged" methods, day-to-day variations of the particle wall-deposition rates are accounted for. Unlike the "size-dependent" method, the "number averaged" and "volume averaged" methods assume that particle wall-deposition rates depend weakly on particle size, and hence particle wall-deposition can be represented by a single first-order decay rate constant (Carter et al., 2005; Pathak et al., 2007; Pierce et al., 2008). It is currently unclear if this assumption is valid for all seed aerosol concentrations (i.e., number, surface area and volume concentrations). The "inert tracer" method can be used in SOA-formation studies where SMPS and AMS measurements are taken and non-

Atmos. Chem. Phys. Discuss., doi:10.5194/acp-2016-820, 2016
Manuscript under review for journal Atmos. Chem. Phys.
Published: 19 September 2016

457 volatile sulfate seed aerosol is used (Hildebrandt et al., 2009). The SOA mass
458 concentration is calculated from the product of the initial seed aerosol sulfate mass
459 concentration (measured by the SMPS) to the time-dependent organic-to-sulfate
460 (Org/SO_4) ratio (measured by the HR-ToF-AMS). Examples of the application of the
461 "number averaged", "volume averaged" and "inert tracer" methods to the α-pinene
462 ozonolysis data are shown in Fig. S7.

463 In original descriptions of the "size-dependent", "number average" and "volume
464 average" methods, the authors assumed that particles cease to uptake SOA-forming
465 vapors once they have deposited to the walls, thus the SOA mass present on deposited
466 particles does not increase after deposition (Carter et al., 2005; Pathak et al., 2007; Loza
467 et al., 2012). In contrast, the "inert tracer" method assumes that deposited particles
468 continue to uptake suspended SOA-forming vapors at similar rates as suspended
469 particles, and hence the SOA mass present on the deposited particles will increase at the
470 same rate as those suspended (Hildebrandt et al., 2009). Therefore, SOA mass
471 concentrations and yields calculated by the "inert tracer" method are expected to be
472 higher than that calculated using the original descriptions of the "size-dependent",
473 "number average" and "volume average" methods. It is important to note that the
474 assumption that deposited particles continue to uptake suspended SOA-forming vapors at
475 similar rates as suspended particles can also be applied to the "size-dependent", "number
476 average" and "volume average" methods, which in turn will result in higher calculated
477 SOA mass concentrations and yields. However, we will use the "size-dependent",
478 "number average" and "volume average" methods as originally described by Loza et al.
479 (2012), Carter et al. (2005) and Pathak et al. (2007), respectively, to correct for particle
480 wall-deposition in this discussion (i.e., deposited particles do not uptake SOA-forming
481 vapors). The "inert tracer" method will be used to evaluate its ability to predict the role of
482 gas-particle partitioning (quasi-equilibrium vs. kinetically limited SOA growth) in
483 affecting vapor wall-deposition and SOA mass yields in the α-pinene ozonolysis system.

484 Figure 5 shows the SOA mass concentrations as a function of reaction time for the
485 four particle wall-deposition correction methods. For the low-SA experiments (Figs. 5a
486 and 5b), the SOA growth profiles obtained using the four different particle wall-

Atmos. Chem. Phys. Discuss., doi:10.5194/acp-2016-820, 2016
Manuscript under review for journal Atmos. Chem. Phys.
Published: 19 September 2016

deposition correction methods are similar; SOA growth virtually stops after all the α-pinene has reacted (at reaction time ~90 to 100 min). As expected, the SOA mass concentrations calculated by the "inert tracer" method are higher than the SOA mass concentrations calculated by the "size-dependent", "number averaged" and "volume averaged" methods. The SOA mass concentrations calculated by the "size-dependent", "number averaged" and "volume averaged" particle wall-deposition methods are generally consistent with each other.

For the high-SA experiments (Figs. 5c to 5f), the SOA mass concentrations calculated using the "size-dependent", "volume averaged" and "inert tracer" methods stop increasing after all the α-pinene has reacted (at reaction time ~90 to 100 min). In contrast, the SOA mass concentrations calculated using the "number averaged" method continued to increase even after all the α-pinene has reacted. These results suggest that the calculated SOA mass concentrations and yields will be substantially overestimated if the "number averaged" method is used to correct for particle wall-deposition in experiments where high seed aerosol surface area concentrations are used. The erroneous increase in the SOA mass concentration calculated by the "number averaged" method can be attributed to the method's assumption that the average loss rate of the total aerosol volume concentration is the same as that of the total aerosol number concentration. The "number averaged" method is effective in experiments where low concentrations of seed aerosol are used since coagulation plays a minor role in affecting the average loss rate of the total aerosol number concentration. However, it loses its accuracy in experiments where high concentrations of seed aerosol are used because the average loss rate of the total aerosol number concentration is driven by both coagulation and particle wall-deposition. It is possible that the "number averaged" method may be an effective particle wall-deposition correction method in these experiments if the measurements are corrected for coagulation. The effect of coagulation on the SOA mass concentrations calculated by the "volume averaged" and "inert tracer" methods is less prominent since coagulation does not affect the aerosol volume and mass concentrations. Together, our results indicate that the "size-dependent" (when coagulation is accounted for), "volume averaged" and "inert tracer" methods are effective particle wall-deposition correction methods

Atmos. Chem. Phys. Discuss., doi:10.5194/acp-2016-820, 2016
Manuscript under review for journal Atmos. Chem. Phys.
Published: 19 September 2016

(regardless of seed aerosol surface area concentrations) since the calculated SOA mass concentrations stopped increasing after all the α-pinene has reacted.

Figure 6 shows the time-dependent SOA mass yields as a function of initial total AS seed aerosol surface area concentration for the "number averaged", "volume averaged" and "inert tracer" particle wall-deposition correction methods. Also shown in Fig. 6 are time-dependent SOA mass yields calculated using these three methods for the α-pinene ozonolysis raw data reported by Nah et al. (2016). The time-dependent SOA mass yields for the "number averaged", "volume averaged" and "inert tracer" methods (Fig. 6) are compared to those calculated using the "size-dependent" method (Fig. 4). For seed aerosol surface area concentrations < 3000 μm^2 cm^{-3}, the SOA mass yields at peak SOA growth (absolute values) calculated by the "size-dependent", "number averaged" and "volume averaged" methods agree within 14 % (Figs. 4, 6a and 6b). In contrast, for seed aerosol surface area concentrations ≥ 8000 μm^2 cm^{-3}, the SOA mass yields at peak SOA growth calculated by the "number averaged" method range from 70.8 to 76.5 % (Fig. 6a), while SOA mass yields at peak SOA growth calculated by the "size-dependent" and "volume average" methods range from 17.2 to 27 % (Figs. 4 and 6b). As discussed previously, this disagreement in the SOA mass yields is due to the treatment of (or lack thereof) coagulation in the "number averaged" method. Failure to account for coagulation in the "number averaged" method also resulted in the calculated SOA mass yields increasing with seed aerosol surface area (Fig. 6a), which could lead to the incorrect conclusion that SOA formation in the α-pinene ozonolysis system is governed by kinetically limited growth. In contrast, the SOA mass yields calculated by the "volume averaged" and "inert tracer" methods remain roughly constant despite the increase in AS seed aerosol surface area (Figs. 6b and 6c), consistent with the results obtained using the "size-dependent" method (Fig. 4).

5. Conclusions

An aerosol dynamics model can be used to account for coagulation in chamber studies in which large seed aerosol surface area concentrations are used. Coagulation-corrected size-dependent particle wall-deposition coefficients are obtained from the application of the aerosol dynamics model to the experimental data from seed-only

Atmos. Chem. Phys. Discuss., doi:10.5194/acp-2016-820, 2016
Manuscript under review for journal Atmos. Chem. Phys.
Published: 19 September 2016

547 experiments. Using these coagulation-corrected size-dependent particle wall-deposition
548 coefficients, we showed that the α-pinene ozonolysis SOA mass yields at peak SOA
549 growth remain approximately constant even when very high seed aerosol surface area
550 concentrations (≥ 8000 μm^2 cm^{-3}) are used. This confirms conclusions from our previous
551 study that the seed aerosol surface area concentration does not influence the partitioning
552 of α-pinene ozonolysis gas-phase products to the particle phase (Nah et al., 2016). Thus,
553 this indicates that SOA formation in the α-pinene ozonolysis system is dominated by
554 quasi-equilibrium growth, and that there are no significant limitations to vapor-particle
555 mass transfer (McVay et al., 2014; Nah et al., 2016).

556 The variability in the calculated SOA mass concentrations and yields between
557 four different particle wall-deposition correction methods is also evaluated for a series of
558 α-pinene ozonolysis experiments. In the experiments with low seed aerosol surface area
559 concentrations (< 3000 μm^2 cm^{-3}), the SOA mass yields obtained by the different particle
560 wall-deposition correction methods are generally consistent with one another. However,
561 in the experiments with high seed aerosol surface area concentrations (≥ 8000 μm^2 cm^{-3}),
562 the calculated SOA mass yields differ substantially. These differences arise from
563 assumptions made in the particle wall-deposition correction method regarding the
564 influence of coagulation on the first-order particle wall-loss rate.

565 Chamber experiments are subject to both particle and vapor wall-deposition.
566 While understanding the effect of vapor wall-deposition on the SOA mass yields is
567 critical, SOA mass yield uncertainties introduced by the particle wall-deposition
568 correction cannot be neglected. Results from this study underscore the importance of
569 constraining the SOA mass yield uncertainties introduced by the particle wall-deposition
570 correction regardless of the VOC system. Specifically, the effect of coagulation on
571 particle wall-deposition rates can be an important source of uncertainty not only in
572 determining SOA mass concentrations and yields, but also in evaluating the role of gas-
573 particle partitioning (quasi-equilibrium vs. kinetically limited SOA growth) in affecting
574 vapor wall-deposition in VOC systems. Here we showed that the condensation of SOA-
575 forming vapors in the α-pinene ozonolysis system can be erroneously concluded as
576 kinetically limited if coagulation is not accounted for in the "size-dependent" and

577 "number averaged" particle wall-deposition correction methods. Similar flawed
578 conclusions in other VOC systems may be drawn in chamber studies that use high seed
579 aerosol surface area concentrations to promote SOA formation but do not account for
580 coagulation. Therefore, we recommend accounting for coagulation when the "size-
581 dependent" and "number averaged" particle wall-deposition correction methods are used
582 in chamber studies that use high seed aerosol surface area concentrations (i.e., ≥ 3000
583 μm^2 cm^{-3}) to promote the condensation of SOA-forming vapors onto seed aerosol
584 regardless of VOC system. Alternatively, the "volume averaged" and "inert tracer"
585 methods can be used in chamber studies that use high seed aerosol surface area
586 concentrations. In addition, we suggest using multiple techniques (i.e., at least 2) to
587 correct for particle wall-loss in order to determine the effect of SOA mass yield
588 uncertainties introduced by particle wall-deposition correction.

589 It is important to note that while results from the present study indicate that the
590 "volume dependent" and "inert tracer" methods are appropriate particle wall-deposition
591 correction methods for SOA-formation studies (regardless of seed aerosol surface area
592 concentrations) performed in the GTEC chamber in which the particle wall-loss rates
593 strongly depend on particle size, this may not be the case for all chambers. In addition to
594 particle size, particle wall-deposition rates depend on the chamber geometry, chamber
595 turbulence induced by mixing, and charge distribution on particles (Crump and Seinfeld,
596 1981; McMurry and Rader, 1985). All these factors need to be considered before one
597 decides which particle wall-deposition correction method to use in SOA-formation
598 studies. It is possible that the "volume dependent" and "inert tracer" methods may not be
599 appropriate particle wall-deposition correction methods for SOA-formation studies
600 performed in a chamber in which the particle wall-loss rates are even more strongly
601 dependent on particle size compared to the GTEC chamber. Therefore, we recommend
602 performing at least one separate seed-only experiment to measure the size-dependent
603 particle wall-deposition coefficients in order to probe the particle wall-deposition
604 characteristics of the chamber used before deciding on the particle wall-deposition
605 method to use in SOA-formation studies.

606 **Acknowledgements**

This research was funded by NSF grants 1455588 and AGS-1523500, and US Environmental Protection Agency STAR grant (Early Career) RD-83540301. This publication's contents are solely the responsibility of the grantee and do not necessarily represent the official views of the US EPA. Further, US EPA does not endorse the purchase of any commercial products or services mentioned in the publication. R.C. McVay was supported by a National Science Foundation Graduate Research Fellowship under grant No. DGE-1144469.

References

Boyd, C. M., Sanchez, J., Xu, L., Eugene, A. J., Nah, T., Tuet, W. Y., Guzman, M. I., and Ng, N. L.: Secondary organic aerosol formation from the β-pinene+NO3 system: effect of humidity and peroxy radical fate, Atmos. Chem. Phys., 15, 7497-7522, 10.5194/acp-15-7497-2015, 2015.

Canagaratna, M. R., Jimenez, J. L., Kroll, J. H., Chen, Q., Kessler, S. H., Massoli, P., Hildebrandt Ruiz, L., Fortner, E., Williams, L. R., Wilson, K. R., Surratt, J. D., Donahue, N. M., Jayne, J. T., and Worsnop, D. R.: Elemental ratio measurements of organic compounds using aerosol mass spectrometry: characterization, improved calibration, and implications, Atmos. Chem. Phys., 15, 253-272, 10.5194/acp-15-253-2015, 2015.

Cappa, C. D., Jathar, S. H., Kleeman, M. J., Docherty, K. S., Jimenez, J. L., Seinfeld, J. H., and Wexler, A. S.: Simulating secondary organic aerosol in a regional air quality model using the statistical oxidation model – Part 2: Assessing the influence of vapor wall losses, Atmos. Chem. Phys., 16, 3041-3059, 10.5194/acp-16-3041-2016, 2016.

Carter, W. P. L., Cocker, D. R., Fitz, D. R., Malkina, I. L., Bumiller, K., Sauer, C. G., Pisano, J. T., Bufalino, C., and Song, C.: A new environmental chamber for evaluation of gas-phase chemical mechanisms and secondary aerosol formation, Atmospheric Environment, 39, 7768-7788, 10.1016/j.atmosenv.2005.08.040, 2005.

Chan, A. W. H., Kroll, J. H., Ng, N. L., and Seinfeld, J. H.: Kinetic modeling of secondary organic aerosol formation: effects of particle- and gas-phase reactions of semivolatile products, Atmospheric Chemistry and Physics, 7, 4135-4147, 2007.

635 Cocker, D. R., Flagan, R. C., and Seinfeld, J. H.: State-of-the-art chamber facility for
636 studying atmospheric aerosol chemistry, Environmental Science & Technology, 35,
637 2594-2601, 10.1021/es0019169, 2001.

638 Crump, J. G., and Seinfeld, J. H.: Turbulent Deposition and Gravitational Sedimentation
639 of an Aerosol in a Vessel of Arbitrary Shape, Journal of Aerosol Science, 12, 405-415,
640 10.1016/0021-8502(81)90036-7, 1981.

641 DeCarlo, P. F., Kimmel, J. R., Trimborn, A., Northway, M. J., Jayne, J. T., Aiken, A. C.,
642 Gonin, M., Fuhrer, K., Horvath, T., Docherty, K. S., Worsnop, D. R., and Jimenez, J. L.:
643 Field-deployable, high-resolution, time-of-flight aerosol mass spectrometer, Analytical
644 Chemistry, 78, 8281-8289, 10.1021/ac061249n, 2006.

645 Hallquist, M., Wenger, J. C., Baltensperger, U., Rudich, Y., Simpson, D., Claeys, M.,
646 Dommen, J., Donahue, N. M., George, C., Goldstein, A. H., Hamilton, J. F., Herrmann,
647 H., Hoffmann, T., Iinuma, Y., Jang, M., Jenkin, M. E., Jimenez, J. L., Kiendler-Scharr,
648 A., Maenhaut, W., McFiggans, G., Mentel, T. F., Monod, A., Prevot, A. S. H., Seinfeld,
649 J. H., Surratt, J. D., Szmigielski, R., and Wildt, J.: The formation, properties and impact
650 of secondary organic aerosol: current and emerging issues, Atmospheric Chemistry and
651 Physics, 9, 5155-5236, 2009.

652 Hildebrandt, L., Donahue, N. M., and Pandis, S. N.: High formation of secondary organic
653 aerosol from the photo-oxidation of toluene, Atmospheric Chemistry and Physics, 9,
654 2973-2986, 2009.

655 Kanakidou, M., Seinfeld, J. H., Pandis, S. N., Barnes, I., Dentener, F. J., Facchini, M. C.,
656 Van Dingenen, R., Ervens, B., Nenes, A., Nielsen, C. J., Swietlicki, E., Putaud, J. P.,
657 Balkanski, Y., Fuzzi, S., Horth, J., Moortgat, G. K., Winterhalter, R., Myhre, C. E. L.,
658 Tsigaridis, K., Vignati, E., Stephanou, E. G., and Wilson, J.: Organic aerosol and global
659 climate modelling: a review, Atmospheric Chemistry and Physics, 5, 1053-1123, 2005.

660 Keywood, M. D., Varutbangkul, V., Bahreini, R., Flagan, R. C., and Seinfeld, J. H.:
661 Secondary organic aerosol formation from the ozonolysis of cycloalkenes and related

662 compounds, Environmental Science & Technology, 38, 4157-4164, 10.1021/es035363o,
663 2004.

664 Kokkola, H., Yli-Pirila, P., Vesterinen, M., Korhonen, H., Keskinen, H., Romakkaniemi,
665 S., Hao, L., Kortelainen, A., Joutsensaari, J., Worsnop, D. R., Virtanen, A., and Lehtinen,
666 K. E. J.: The role of low volatile organics on secondary organic aerosol formation,
667 Atmospheric Chemistry and Physics, 14, 1689-1700, 10.5194/acp-14-1689-2014, 2014.

668 Krechmer, J. E., Pagonis, D., Ziemann, P. J., and Jimenez, J. L.: Quantification of Gas-
669 Wall Partitioning in Teflon Environmental Chambers Using Rapid Bursts of Low-
670 Volatility Oxidized Species Generated in Situ, Environmental Science & Technology, 50,
671 5757-5765, 10.1021/acs.est.6b00606, 2016.

672 Kroll, J. H., and Seinfeld, J. H.: Chemistry of secondary organic aerosol: Formation and
673 evolution of low-volatility organics in the atmosphere, Atmospheric Environment, 42,
674 3593-3624, 10.1016/j.atmosenv.2008.01.003, 2008.

675 La, Y. S., Camredon, M., Ziemann, P. J., Valorso, R., Matsunaga, A., Lannuque, V., Lee-
676 Taylor, J., Hodzic, A., Madronich, S., and Aumont, B.: Impact of chamber wall loss of
677 gaseous organic compounds on secondary organic aerosol formation: explicit modeling
678 of SOA formation from alkane and alkene oxidation, Atmos. Chem. Phys., 16, 1417-
679 1431, 10.5194/acp-16-1417-2016, 2016.

680 Loza, C. L., Chan, A. W. H., Galloway, M. M., Keutsch, F. N., Flagan, R. C., and
681 Seinfeld, J. H.: Characterization of Vapor Wall Loss in Laboratory Chambers,
682 Environmental Science & Technology, 44, 5074-5078, 10.1021/es100727v, 2010.

683 Loza, C. L., Chhabra, P. S., Yee, L. D., Craven, J. S., Flagan, R. C., and Seinfeld, J. H.:
684 Chemical aging of m-xylene secondary organic aerosol: laboratory chamber study,
685 Atmospheric Chemistry and Physics, 12, 151-167, 10.5194/acp-12-151-2012, 2012.

686 Matsunaga, A., and Ziemann, P. J.: Gas-Wall Partitioning of Organic Compounds in a
687 Teflon Film Chamber and Potential Effects on Reaction Product and Aerosol Yield

688 Measurements, Aerosol Science and Technology, 44, 881-892,
689 10.1080/02786826.2010.501044, 2010.

690 McMurry, P. H., and Grosjean, D.: Gas and Aerosol Wall Losses in Teflon Film Smog
691 Chambers, Environmental Science & Technology, 19, 1176-1182, 10.1021/es00142a006,
692 1985.

693 McMurry, P. H., and Rader, D. J.: Aerosol Wall Losses in Electrically Charged
694 Chambers, Aerosol Science and Technology, 4, 249-268, 10.1080/02786828508959054,
695 1985.

696 McVay, R. C., Cappa, C. D., and Seinfeld, J. H.: Vapor-Wall Deposition in Chambers:
697 Theoretical Considerations, Environmental Science & Technology, 48, 10251-10258,
698 10.1021/es502170j, 2014.

699 McVay, R. C., Zhang, X., Aumont, B., Valorso, R., Camredon, M., La, Y. S., Wennberg,
700 P. O., and Seinfeld, J. H.: SOA formation from the photooxidation of α-pinene:
701 systematic exploration of the simulation of chamber data, Atmos. Chem. Phys., 16, 2785-
702 2802, 10.5194/acp-16-2785-2016, 2016.

703 Nah, T., McVay, R. C., Zhang, X., Boyd, C. M., Seinfeld, J. H., and Ng, N. L.: Influence
704 of seed aerosol surface area and oxidation rate on vapor wall deposition and SOA mass
705 yields: a case study with α-pinene ozonolysis, Atmos. Chem. Phys., 16, 9361-9379,
706 10.5194/acp-16-9361-2016, 2016.

707 Ng, N. L., Kroll, J. H., Keywood, M. D., Bahreini, R., Varutbangkul, V., Flagan, R. C.,
708 Seinfeld, J. H., Lee, A., and Goldstein, A. H.: Contribution of first- versus second-
709 generation products to secondary organic aerosols formed in the oxidation of biogenic
710 hydrocarbons, Environmental Science & Technology, 40, 2283-2297,
711 10.1021/es052269u, 2006.

712 Odum, J. R., Hoffmann, T., Bowman, F., Collins, D., Flagan, R. C., and Seinfeld, J. H.:
713 Gas/Particle Partitioning and Secondary Organic Aerosol Yields, Environmental Science
714 & Technology, 30, 2580-2585, 10.1021/es950943+, 1996.

715 Odum, J. R., Jungkamp, T. P. W., Griffin, R. J., Flagan, R. C., and Seinfeld, J. H.: The
716 atmospheric aerosol-forming potential of whole gasoline vapor, Science, 276, 96-99,
717 10.1126/science.276.5309.96, 1997a.

718 Odum, J. R., Jungkamp, T. P. W., Griffin, R. J., Forstner, H. J. L., Flagan, R. C., and
719 Seinfeld, J. H.: Aromatics, reformulated gasoline, and atmospheric organic aerosol
720 formation, Environmental Science & Technology, 31, 1890-1897, 10.1021/es960535l,
721 1997b.

722 Pathak, R. K., Stanier, C. O., Donahue, N. M., and Pandis, S. N.: Ozonolysis of alpha-
723 pinene at atmospherically relevant concentrations: Temperature dependence of aerosol
724 mass fractions (yields), J. Geophys. Res.-Atmos., 112, 8, 10.1029/2006jd007436, 2007.

725 Pierce, J. R., Engelhart, G. J., Hildebrandt, L., Weitkamp, E. A., Pathak, R. K., Donahue,
726 N. M., Robinson, A. L., Adams, P. J., and Pandis, S. N.: Constraining particle evolution
727 from wall losses, coagulation, and condensation-evaporation in smog-chamber
728 experiments: Optimal estimation based on size distribution measurements, Aerosol
729 Science and Technology, 42, 1001-1015, 10.1080/02786820802389251, 2008.

730 Riipinen, I., Pierce, J. R., Yli-Juuti, T., Nieminen, T., Häkkinen, S., Ehn, M., Junninen,
731 H., Lehtipalo, K., Petäjä, T., Slowik, J., Chang, R., Shantz, N. C., Abbatt, J., Leaitch, W.
732 R., Kerminen, V. M., Worsnop, D. R., Pandis, S. N., Donahue, N. M., and Kulmala, M.:
733 Organic condensation: a vital link connecting aerosol formation to cloud condensation
734 nuclei (CCN) concentrations, Atmos. Chem. Phys., 11, 3865-3878, 10.5194/acp-11-3865-
735 2011, 2011.

736 Saleh, R., Donahue, N. M., and Robinson, A. L.: Time Scales for Gas-Particle
737 Partitioning Equilibration of Secondary Organic Aerosol Formed from Alpha-Pinene
738 Ozonolysis, Environmental Science & Technology, 47, 5588-5594, 10.1021/es400078d,
739 2013.

740 Seinfeld, J. H., and Pandis, S. N.: Atmospheric chemistry and physics : from air pollution
741 to climate change, Third edition. ed., John Wiley & Sons, Inc., Hoboken, New Jersey,
742 xxvi, 1120 pages pp., 2016.

743 Shiraiwa, M., and Seinfeld, J. H.: Equilibration timescale of atmospheric secondary
744 organic aerosol partitioning, Geophys. Res. Lett., 39, 6, 10.1029/2012gl054008, 2012.

745 Tsigaridis, K., Daskalakis, N., Kanakidou, M., Adams, P. J., Artaxo, P., Bahadur, R.,
746 Balkanski, Y., Bauer, S. E., Bellouin, N., Benedetti, A., Bergman, T., Berntsen, T. K.,
747 Beukes, J. P., Bian, H., Carslaw, K. S., Chin, M., Curci, G., Diehl, T., Easter, R. C.,
748 Ghan, S. J., Gong, S. L., Hodzic, A., Hoyle, C. R., Iversen, T., Jathar, S., Jimenez, J. L.,
749 Kaiser, J. W., Kirkevåg, A., Koch, D., Kokkola, H., Lee, Y. H., Lin, G., Liu, X., Luo, G.,
750 Ma, X., Mann, G. W., Mihalopoulos, N., Morcrette, J. J., Müller, J. F., Myhre, G.,
751 Myriokefalitakis, S., Ng, N. L., O'Donnell, D., Penner, J. E., Pozzoli, L., Pringle, K. J.,
752 Russell, L. M., Schulz, M., Sciare, J., Seland, Ø., Shindell, D. T., Sillman, S., Skeie, R.
753 B., Spracklen, D., Stavrakou, T., Steenrod, S. D., Takemura, T., Tiitta, P., Tilmes, S.,
754 Tost, H., van Noije, T., van Zyl, P. G., von Salzen, K., Yu, F., Wang, Z., Wang, Z.,
755 Zaveri, R. A., Zhang, H., Zhang, K., Zhang, Q., and Zhang, X.: The AeroCom evaluation
756 and intercomparison of organic aerosol in global models, Atmos. Chem. Phys., 14,
757 10845-10895, 10.5194/acp-14-10845-2014, 2014.

758 Weitkamp, E. A., Sage, A. M., Pierce, J. R., Donahue, N. M., and Robinson, A. L.:
759 Organic aerosol formation from photochemical oxidation of diesel exhaust in a smog
760 chamber, Environmental Science & Technology, 41, 6969-6975, 10.1021/es070193r,
761 2007.

762 Ye, P., Ding, X., Hakala, J., Hofbauer, V., Robinson, E. S., and Donahue, N. M.: Vapor
763 wall loss of semi-volatile organic compounds in a Teflon chamber, Aerosol Science and
764 Technology, 50, 822-834, 10.1080/02786826.2016.1195905, 2016.

765 Yeh, G. K., and Ziemann, P. J.: Alkyl Nitrate Formation from the Reactions of C-8-C-14
766 n-Alkanes with OH Radicals in the Presence of NOx: Measured Yields with Essential
767 Corrections for Gas-Wall Partitioning, J. Phys. Chem. A, 118, 8147-8157,
768 10.1021/jp500631v, 2014.

769 Yeh, G. K., and Ziemann, P. J.: Gas-Wall Partitioning of Oxygenated Organic
770 Compounds: Measurements, Structure-Activity Relationships, and Correlation with Gas

771 Chromatographic Retention Factor, Aerosol Science and Technology, 49, 726-737,
772 10.1080/02786826.2015.1068427, 2015.

773 Zhang, X., Pandis, S. N., and Seinfeld, J. H.: Diffusion-Limited Versus Quasi-
774 Equilibrium Aerosol Growth, Aerosol Science and Technology, 46, 874-885,
775 10.1080/02786826.2012.679344, 2012.

776 Zhang, X., Cappa, C. D., Jathar, S. H., McVay, R. C., Ensberg, J. J., Kleeman, M. J., and
777 Seinfeld, J. H.: Influence of vapor wall loss in laboratory chambers on yields of
778 secondary organic aerosol, Proc. Natl. Acad. Sci. U. S. A., 111, 5802-5807,
779 10.1073/pnas.1404727111, 2014.

780 Zhang, X., Schwantes, R. H., McVay, R. C., Lignell, H., Coggon, M. M., Flagan, R. C.,
781 and Seinfeld, J. H.: Vapor wall deposition in Teflon chambers, Atmospheric Chemistry
782 and Physics, 15, 4197-4214, 10.5194/acp-15-4197-2015, 2015.
783

784

785

786

787

788

789

790

791

792

793

794

Atmos. Chem. Phys. Discuss., doi:10.5194/acp-2016-820, 2016
Manuscript under review for journal Atmos. Chem. Phys.
Published: 19 September 2016

Atmospheric Chemistry and Physics Discussions

795 **Table 1:** Experimental conditions and results

Expt	Experimental Conditions	Initial Seed aerosol Surface area ($\mu m^2\ cm^{-3}$)	Initial [α-pinene][a] ($\mu g\ m^{-3}$)	ΔM_o[b,c] ($\mu g\ m^{-3}$)	SOA Mass Yield[d] (%)
1	0.015 M AS, seed only[e]	1090	-	-	-
2	0.05 M AS, seed only[e]	1190	-	-	-
3	0.015 M & 0.05 M AS, seed only[e]	1470	-	-	-
4	0.015 M & 0.05 M AS, seed only[e]	1210	-	-	-
5	0.05 M AS, seed only[f]	8000	-	-	-
6	0.015 M & 0.05 M AS, seed only[f]	8580	-	-	-
7	0.015 M AS, O_3+α-pinene[g,i]	1090	281.8±14.9	71.5±0.5	25.4±1.3
8	0.05 M AS, O_3+α-pinene[g,j]	1260	278.5±13.9	65.9±0.9	23.7±1.2
9	0.05 M AS, O_3+α-pinene[h,k]	9160	283.8±14.2	74.2±1.9	26.1±1.5
10	0.05 M AS, O_3+α-pinene[h,k]	8390	265.8±13.3	71.0±3.4	26.7±1.9
11	0.015 M & 0.05 M AS, O_3+α-pinene[h,l]	8180	289.8±14.5	60.5±1.7	20.9±1.2
12	0.015 M & 0.05 M AS, O_3+α-pinene[h,l]	9440	271.8±13.6	53.7±2.9	19.7±1.4

796 [a]All the α-pinene reacted in the 500 ppb O_3 experiments.
797 [b]The SOA mass concentration (ΔM_o) is calculated using the density = 1.37 g cm^{-3}
798 obtained from the 500 ppb O_3 nucleation experiment in Nah et al. (2016).
799 [c]Uncertainties in the peak SOA mass concentration are calculated from one standard
800 deviation of the aerosol volume as measured by the scanning mobility particle sizer.
801 [d]SOA mass yields at peak SOA growth are reported.
802 [e]Referred to as a "low-SA-seed-only experiment" in the main text.
803 [f]Referred to as a "high-SA-seed-only experiment" in the main text.
804 [g]Referred to as a "low-SA experiment" in the main text.
805 [h]Referred to as a "high-SA experiment" in the main text.
806 [i]Size-dependent particle wall-deposition coefficients obtained from Expt 1 were used for
807 particle wall-deposition correction.
808 [j]Size-dependent particle wall-deposition coefficients obtained from Expt 2 were used for
809 particle wall-deposition correction.
810 [k]Size-dependent particle wall-deposition coefficients obtained from Expt 5 were used for
811 particle wall-deposition correction.
812 [l]Size-dependent particle wall-deposition coefficients obtained from Expt 6 were used for
813 particle wall-deposition correction.
814

Atmos. Chem. Phys. Discuss., doi:10.5194/acp-2016-820, 2016
Manuscript under review for journal Atmos. Chem. Phys.
Published: 19 September 2016

Atmospheric Chemistry and Physics Discussions

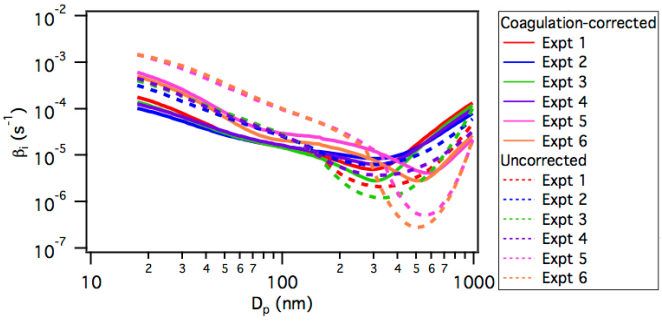

Figure 1: Uncorrected (dashed lines) and coagulation-corrected (solid lines) particle wall-deposition coefficients (β_i) for the low-SA-seed-only (experiments 1 through 4) and high-SA-seed-only (experiments 5 and 6) experiments. Refer to Table 1 for information on the AS solution(s) used to generate the seed aerosol and the initial seed aerosol surface area concentrations in these experiments.

Atmos. Chem. Phys. Discuss., doi:10.5194/acp-2016-820, 2016
Manuscript under review for journal Atmos. Chem. Phys.
Published: 19 September 2016

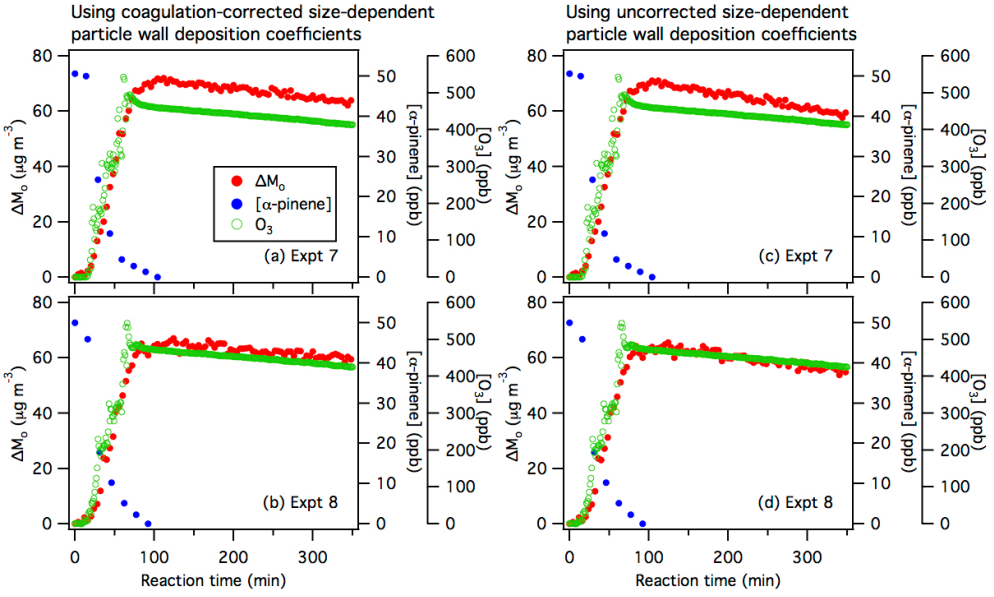

827
828 **Figure 2:** Reaction profiles of the low-SA α-pinene ozonolysis experiments. Panels (a)
829 and (b) show SOA mass concentrations (ΔM_o) obtained using the coagulation-corrected
830 size-dependent particle wall-deposition coefficients from the low-SA-seed-only
831 experiments, while panels (c) and (d) show SOA mass concentrations (ΔM_o) obtained
832 using the uncorrected size-dependent particle wall-deposition coefficients from the low-
833 SA-seed-only experiments. Refer to Table 1 for information on the AS solution(s) used to
834 generate the seed aerosol and the initial seed aerosol surface area concentrations in these
835 experiments.

Atmos. Chem. Phys. Discuss., doi:10.5194/acp-2016-820, 2016
Manuscript under review for journal Atmos. Chem. Phys.
Published: 19 September 2016

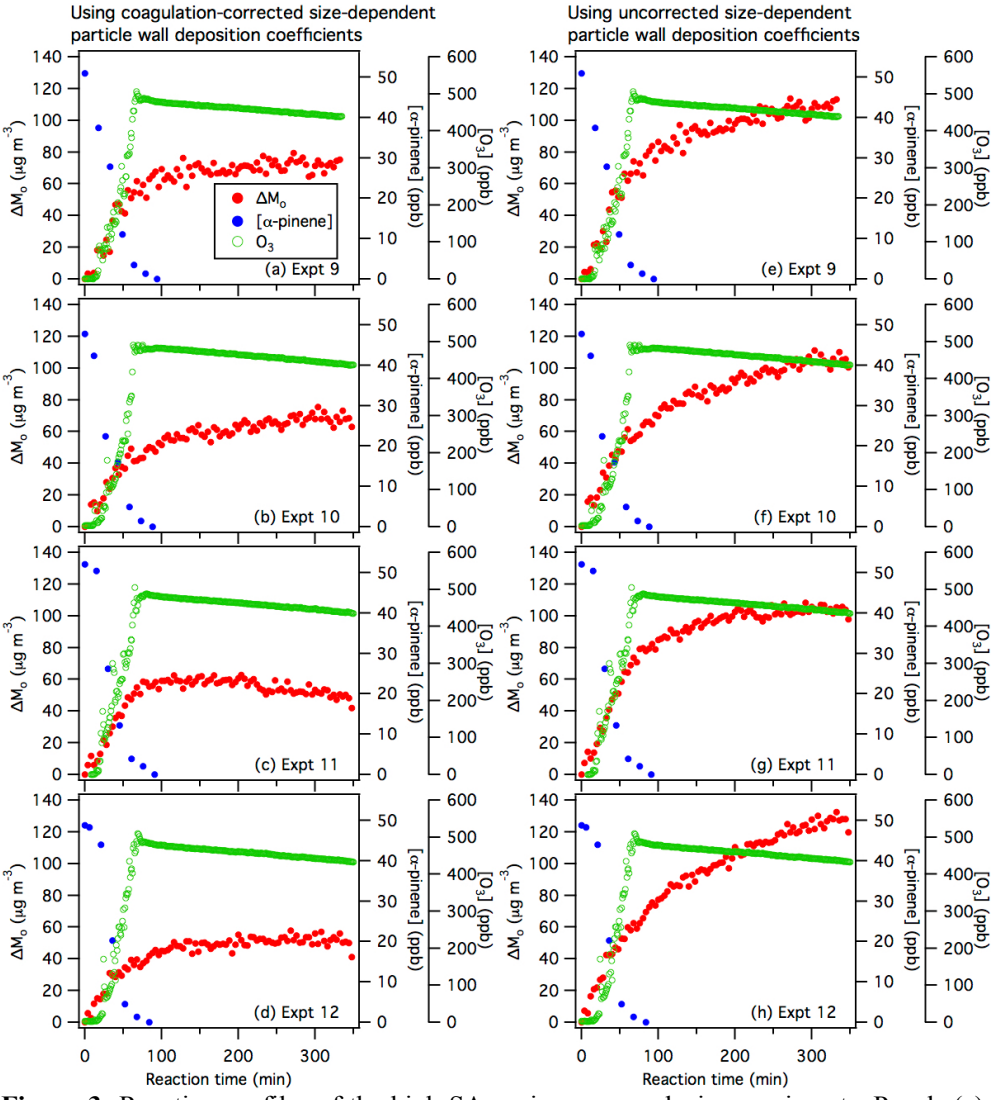

Figure 3: Reaction profiles of the high-SA α-pinene ozonolysis experiments. Panels (a), (b), (c) and (d) show SOA mass concentrations (ΔM_o) obtained using the coagulation-corrected size-dependent particle wall-deposition coefficients from the high-SA-seed-only experiments, while panels (e), (f), (g) and (h) show SOA mass concentrations (ΔM_o) obtained using the uncorrected size-dependent particle wall-deposition coefficients from the high-SA-seed-only experiments. Refer to Table 1 for information on the AS solution(s) used to generate the seed aerosol and the initial seed aerosol surface area concentrations in these experiments. As explained in the main text, SOA mass concentrations are substantially overestimated when the uncorrected size-dependent particle wall-deposition coefficients are used to account for particle wall deposition.

Atmos. Chem. Phys. Discuss., doi:10.5194/acp-2016-820, 2016
Manuscript under review for journal Atmos. Chem. Phys.
Published: 19 September 2016

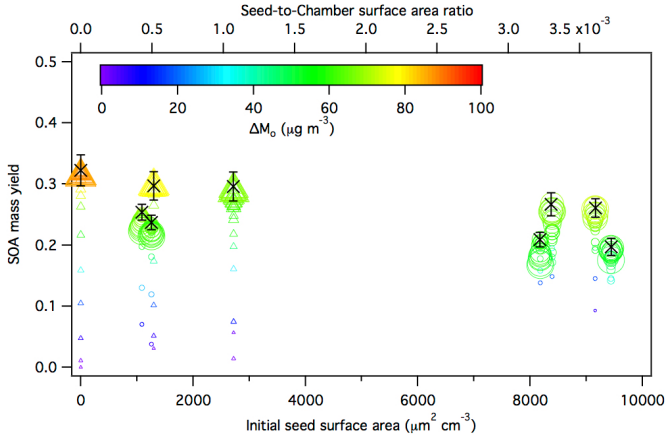

847

848 **Figure 4:** Averaged SOA mass yields over the course of an α-pinene ozonolysis
849 experiment as a function of initial total AS seed aerosol surface area concentration.
850 Results from this study (15 min-averaged) are shown as circles, while results from the
851 study by Nah et al. (2016) (10 min-averaged) are shown as triangles. All the SOA mass
852 yields shown here (including results from Nah et al. (2016)) are obtained using the
853 coagulation-corrected size-dependent particle wall-deposition coefficients. Symbol color
854 indicates the SOA mass concentration and symbol size indicates the time after O_3 is
855 injected into the chamber. The × symbols are the SOA mass yields at peak SOA growth
856 obtained from the experimental data. The y-axis error bars represent the uncertainty in the
857 SOA mass yield at peak SOA growth, which originates from the α-pinene injection and
858 the aerosol mass concentration at peak SOA growth (one standard deviation).

Atmos. Chem. Phys. Discuss., doi:10.5194/acp-2016-820, 2016
Manuscript under review for journal Atmos. Chem. Phys.
Published: 19 September 2016

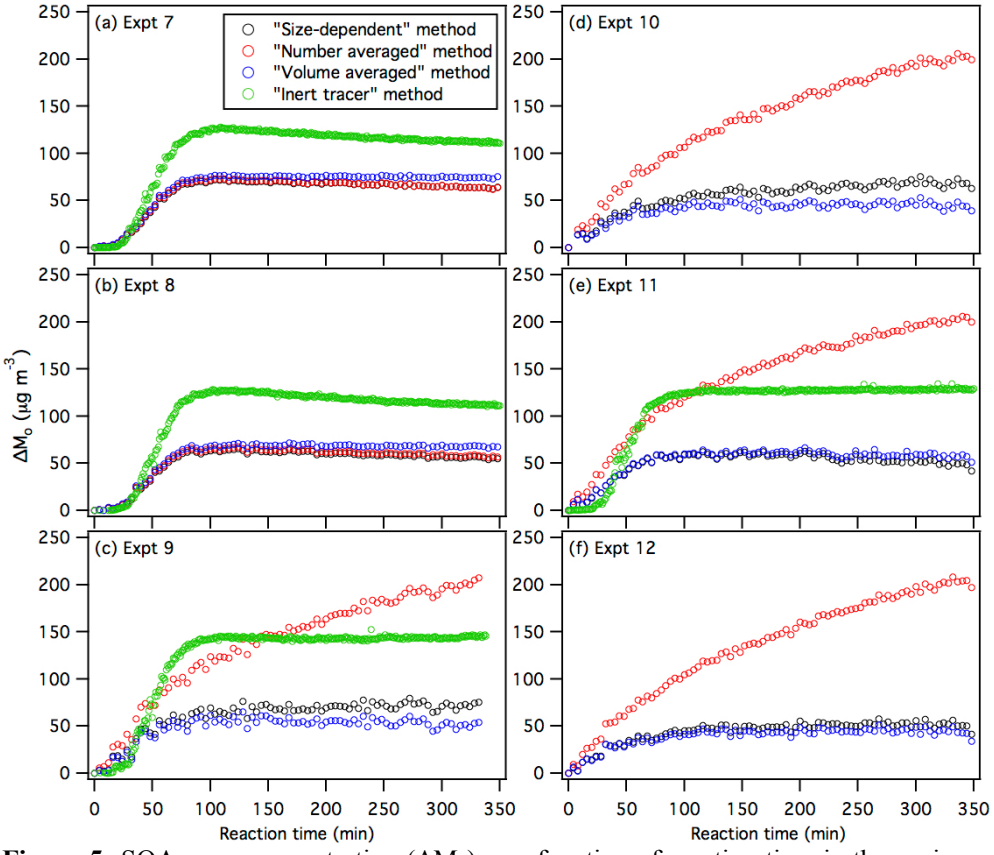

Figure 5: SOA mass concentration (ΔM_o) as a function of reaction time in the α-pinene ozonolysis experiments using the "size-dependent", "number averaged", "volume averaged" and "inert tracer" particle wall-deposition correction methods. HR-ToF-AMS data were not available in experiments 10 and 12, therefore SOA mass concentrations calculated using the "inert tracer" method were not available in these experiments.

Atmos. Chem. Phys. Discuss., doi:10.5194/acp-2016-820, 2016
Manuscript under review for journal Atmos. Chem. Phys.
Published: 19 September 2016

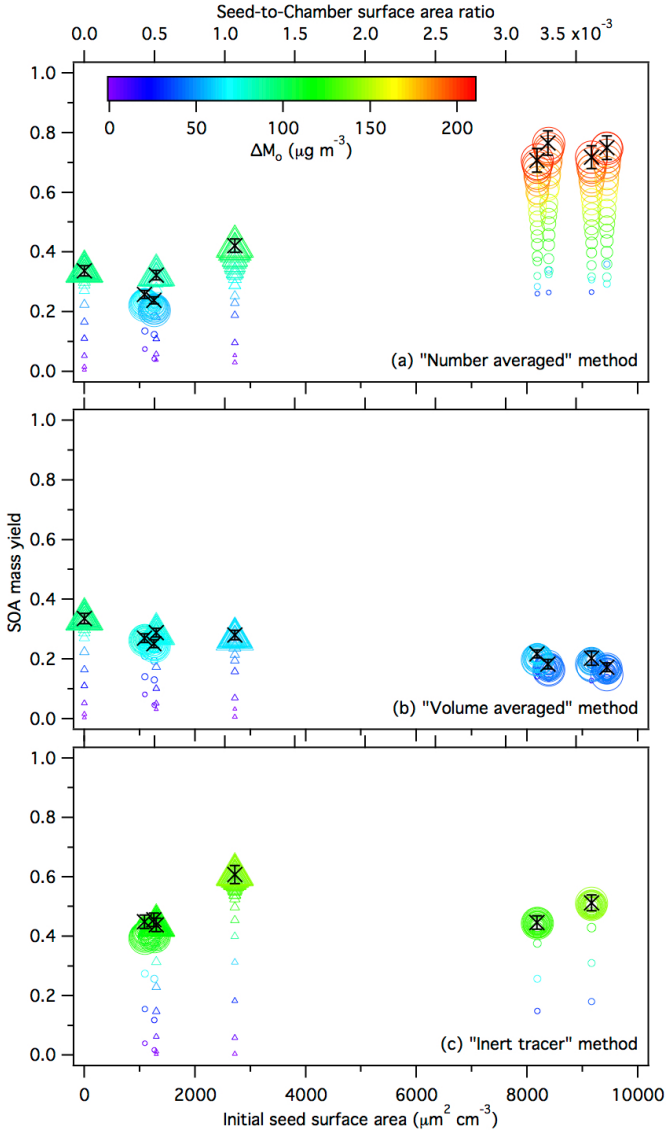

Figure 6: Averaged SOA mass yields over the course of an α-pinene ozonolysis experiment as a function of initial total AS seed aerosol surface area concentration using the (a) "number averaged", (b) "volume averaged" and (c) "inert tracer" particle wall-deposition correction methods. Results from this study (15 min-averaged) are shown as circles, while results from the study by Nah et al. (2016) (10 min-averaged) are shown as triangles. Symbol color indicates the SOA mass concentration and symbol size indicates the time after O_3 is injected into the chamber. The × symbols are the SOA mass yields at peak SOA growth obtained from the experimental data. The y-axis error bars represent the uncertainty in the SOA mass yield at peak SOA growth, which originates from the α-

Atmos. Chem. Phys. Discuss., doi:10.5194/acp-2016-820, 2016
Manuscript under review for journal Atmos. Chem. Phys.
Published: 19 September 2016

875 pinene injection and the aerosol mass concentration at peak SOA growth (one standard
876 deviation).